Figure S3

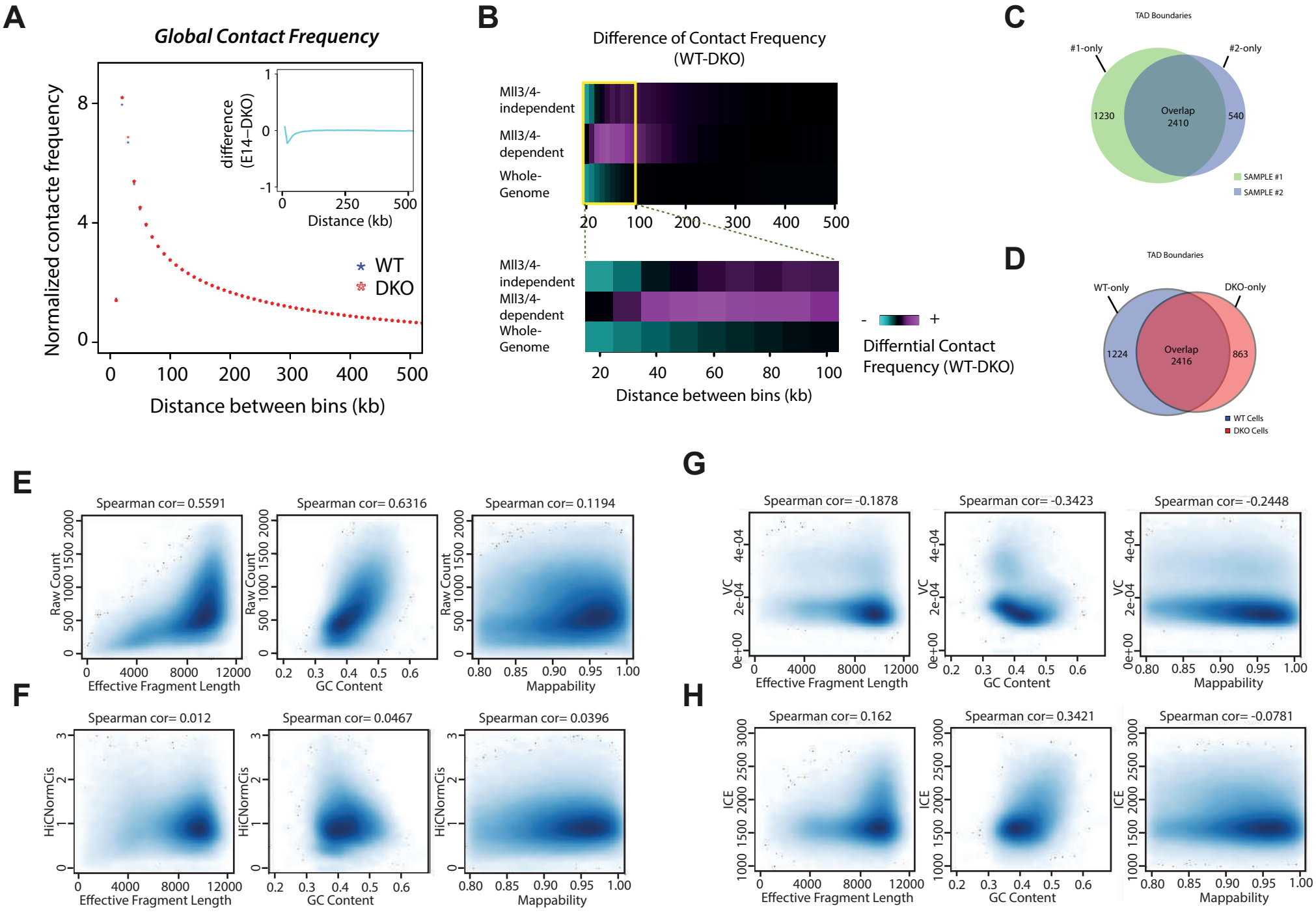
A
Global Contact Frequency
Normalized contacte frequency
Distance between bins (kb)
difference (E14−DKO)
Distance (kb)
WT
DKO
B
Difference of Contact Frequency (WT-DKO)
Mll3/4-independent
Mll3/4-dependent
Whole-Genome
Distance between bins (kb)
Differntial Contact Frequency (WT-DKO)
C
TAD Boundaries
#1-only
#2-only
1230
Overlap 2410
540
SAMPLE #1
SAMPLE #2
D
TAD Boundaries
WT-only
DKO-only
1224
Overlap 2416
863
WT Cells
DKO Cells
E
Spearman cor= 0.5591
Spearman cor= 0.6316
Spearman cor= 0.1194
Raw Count
Effective Fragment Length
GC Content
Mappability
F
Spearman cor= 0.012
Spearman cor= 0.0467
Spearman cor= 0.0396
HiCNormCis
Effective Fragment Length
GC Content
Mappability
G
Spearman cor= -0.1878
Spearman cor= -0.3423
Spearman cor= -0.2448
VC
Effective Fragment Length
GC Content
Mappability
H
Spearman cor= 0.162
Spearman cor= 0.3421
Spearman cor= -0.0781
ICE
Effective Fragment Length
GC Content
Mappability

Figure S3. H3K4me1 does not Affect Global Contact Frequency but is Required for FIREs, Related to Figure 2

(A) Global contact frequency is not obviously affected by Mll3/4 depletion. x-axis shows the distance between two bins. Y-axis is the average value of normalized Hi-C contact frequency. Blue stars, data from WT cells. Red stars, data from DKO cells. Inset shows the subtracted values between two cell types.

(B) Heatmap showing the difference in normalized intra-chromosomal contact frequency at various distance between WT and DKO cells for chromatin regions among different classes of H3K4me1 regions. Mll3/4-independent bins include only Mll3/4-independent H3K4me1 regions; Mll3/4-dependent bins include only Mll3/4-dependent H3K4me1 regions; Whole-Genome, all bins for comparison. Color key shows the normalized differential contact frequency.

(C) Comparison of TAD boundaries between two biological replicates of WT cells. Note that the majority of TAD boundaries are shared by the two samples.

(D) Comparison of TAD boundaries between WT and DKO cells. Note that the difference is of the similar magnitude as biological replicates shown in panel **(C)**.

(E) Scatter plot showing that the raw counts of Hi-C libraries are correlated with fragment length (left), GC content (middle) and mappability (right).

(F) Scatter plot showing after HiCNormCis normalization, the interaction frequency is no longer correlated with the three main bias factors mentioned in **(E).**

(G)-(H) Similar to (**F**), Scatter plot shows after VC or ICE normalization, the interaction frequency is still correlated with the three main bias factors mentioned